Article

Biological Evaluation and Docking Analysis of Potent BACE1 Inhibitors from *Boesenbergia rotunda*

Kumju Youn [1] and **Mira Jun [1,2,3,*]**

[1] Department of Food Science and Nutrition, College of Health Sciences, Dong-A University, 37, Nakdong-daero 550 beon-gil, Saha-gu, Busan 49315, Korea; kjyoun@dau.ac.kr

[2] Center for Silver-Targeted Biomaterials, Brain Busan 21 Plus Program, Graduate School, Dong-A University, Nakdong-daero 550 beon-gil, Saha-gu, Busan 49315, Korea

[3] Institute of Convergence Bio-Health, Dong-A University, Busan 49315, Korea

* Correspondence: mjun@dau.ac.kr; Tel.: +82-51-200-7323

check for updates

Abstract: Alzheimer's disease (AD) is an irreversible neurodegenerative disorder characterized by progressive impairment of cognitive functions. Beta-site amyloid precursor protein cleaving enzyme1 (BACE1) is essential for the formation of β-amyloid peptide (Aβ), a major constituent of amyloid plaques that represent a neuropathological hallmark of this disorder. To find alternative therapies for AD sourced from natural products, the present study focused on three flavonoids from *Boesenbergia rotunda*, namely, cardamonin, pinocembrin, and pinostrobin. Biological evaluation showed that cardamonin presented the strongest BACE1 inhibition, with an The half maximal inhibitory concentration (IC_{50}) value of 4.35 ± 0.38 μM, followed by pinocembrin and pinostrobin with 27.01 ± 2.12 and 28.44 ± 1.96 μM, respectively. Kinetic studies indicated that the inhibitory constants (K_i) for cardamonin, pinocembrin, and pinostrobin against BACE1 were 5.1, 29.3, and 30.9 μM, respectively. Molecular docking studies showed that the tested compounds did not bind to the BACE1 active site, consistent with the biological results, illustrating non-competitive inhibitory activity for all three compounds. In addition, the lowest binding energy of the most proposed complexes of cardamonin, pinocembrin, and pinostrobin with BACE1 were -9.5, -7.9, and -7.6 kcal/mol, respectively. Overall, we provide the first evidence that these flavonoids from *B. rotunda* may be considered as promising AD preventative agents through inhibition of Aβ formation.

Keywords: Alzheimer's disease; Aβ; BACE1; in silico docking; *Boesenbergia rotunda*

1. Introduction

Alzheimer's disease (AD) is an irreversible neurodegenerative disorder that results in progressive behavioral and cognitive impairment. The pathological hallmarks of AD are extracellular beta-amyloid (Aβ) plaque deposits and intracellular neurofibrillary tangles (NFTs) of the microtubule-binding protein tau [1]. Numerous studies strongly support a major role for Aβ aggregates in the initiation phase of AD pathogenesis, although the precise mechanisms of Aβ-induced neurotoxicity remain unclear. Aβ is derived from sequential proteolytic cleavage of the amyloid precursor protein (APP) by two aspartic proteases, β- and γ–secretase. β-Secretase (BACE1) initiates amyloidogenic APP processing, generating sAPPβ and CTF99, and resulting in the processing of CTF99 in the transmembrane region by the γ-secretase complex and then produces the $A\beta_{40}$ and $A\beta_{42}$ peptides [2–4]. Increasing evidence suggests that Aβ generated by BACE1 triggers neuroinflammatory responses by inducing the expression of inflammatory cytokines and mediators via nuclear factor-κB (NF-κB) activation [5]. In addition, reactive oxygen species (ROS) have been revealed to cause the formation of Aβ fibrils, which in turn accelerates oxidative stress, inflammatory responses,

and more Aβ accumulation, ultimately leading to cell death. Recently, it was reported that BACE1 directly contributed to inflammation, indicating that the targeting BACE1 provides suppression of inflammatory responses [6].

Drug discovery efforts aimed at preventing the production of Aβ have focused on targeting the enzymes involved in the amyloidogenic processing of APP. Although several γ-secretase inhibitors have been indicated to inhibit Aβ generation, γ-secretase has a physiologically essential substrate, the Notch signaling protein, which plays a crucial role in the differentiation and proliferation of many cell types [7]. In contrast, BACE1 is a promising alternative for the treatment and/or prevention of AD, considering the relatively mild phenotypes revealed in BACE1-null mice [8,9]. The first generation of BACE1 inhibitors consisted of large peptide-based transition-state analogues, which showed poor in vivo pharmacological properties including a large molecular weight, oral biounavailability, short serum half-life, or low blood–brain barrier (BBB) penetrance [10]. Subsequently, new classes of non-peptidic, lipophilic, small molecule BACE1 inhibitors were designed with improved pharmacological properties. However, these second-generation BACE1 inhibitors were unable to achieve sufficiently high concentrations in the brain due to poor BBB penetration [11]. In contrast, third-generation orally bioavailable BACE1 inhibitors have elicited reduced Aβ production in preclinical animal trials, and some have even entered human clinical trials [12]. The results of several clinical trials showed cerebral Aβ reduction with once-daily oral dosing, although off-target effects, including liver toxicity and skin depigmentation, were also observed [13].

Boesenbergia rotunda (L.) Mansf., also known as fingerroot and Chinese ginger, is widely found in Asian countries including India, Sri Lanka, and southern China. It is commonly used as a food ingredient, as well as in traditional medicine to treat tumors, diarrhea, swelling, and dermatitis [14]. Bioactive *B. rotunda* compounds have been categorized into two major groups, flavanones and chalcones [15]. The main flavanones, like pinocembrin and pinostrobin, and a major chalcone, cardamonin, act as anti-oxidant, anti-inflammatory, anti-tumor, and anti-tuberculosis agents [16]. In addition, these compounds were reported to promote neuroprotective effects against Aβ, glutamate, oxidative stress, inflammation, and ischemic injury in several in vitro and in vivo studies [17–26]. According to the previous research, pinocembrin attenuated 6-OHDA- and Aβ-induced neuronal cell death through the Nrf pathway in SH-SY5Y cells [21,22]. Oral administration of pinocembrin (10 mg/kg) for 7 days suppressed hippocampal inflammation, oxidative stress, and apoptosis in a rat model of global cerebral ischemia-reperfusion [23]. Liu et al. reported that when pinocembrin was orally administered at 20 mg/kg for 8 days, it significantly improved cognitive impairment in intracerebroventricular $Aβ_{25-35}$-injected mice [24]. Moreover, chronic administration of this compound (40 mg/kg) for a 3-month period attenuated cognitive deficits and protected the neurovascular unit in an APP/PS1 transgenic mouse model [25]. Pinostrobin, meanwhile, significantly reduced oxidative stress and mitochondrial-mediated neural apoptosis against Aβ-induced neurotoxicity in PC12 cells [15]. Recently, pinostrobin was also reported to improve neuronal cell loss and deficient locomotive behavior induced by 1-methyl-4-phenyl-1,2,3,6-tetrahydropyridine (MPTP) in zebrafish, and to protect SH-SY6Y cells against 1-methyl-4-phenylpyridinium (MPP+)-induced oxidative stress and apoptosis, suggesting that pinostrobin has neuroprotective potential both in vitro and in vivo [26]. Although cardamonin is the least studied of the three flavanones, it was shown to afford neuroprotection against oxidative injury in PC12 cells and to inhibit neuroinflammation in the mouse microglia BV2 cell line [18,19].

The three compounds from *B. rotunda* were proven to possess anti-inflammatory properties in neuronal cell models, suggesting that these three compounds might regulate inflammatory response by way of suppressing BACE1 activation. Therefore, in the present study, for the first time, the direct effects of these compounds against BACE1 were examined through in vitro and in silico docking approaches.

2. Materials and Methods

2.1. Reagents

Cardamonin (>98%), pinocembrin (>95%), pinostrobin (>99%), trans-resveratrol (>99%), chymotrypsin, trypsin, elastase, and their substrates were purchased from Sigma-Aldrich (St. Louis, MO, USA). The BACE1 assay kit was purchased from Invitrogen (Pan Vera, Madison, WI, USA). Tumor necrosis factor- α converting enzyme (TACE), a major α-secretase, and its substrate were bought from R&D Systems (Minneapolis, MN, USA).

2.2. In Vitro Enzyme Inhibitory Assay for Biological Evaluation

Enzyme assays for BACE1, TACE, chymotrypsin, trypsin, and elastase were carried out according to previously described methods [27]. Briefly, reaction mixtures containing human recombinant BACE1 (1.0 U/mL), a specific substrate (Rh-EVNLDAEFK-Quencher in 50 mM ammonium bicarbonate), and samples dissolved in an assay buffer (50 mM sodium acetate, pH 4.5) were incubated for 60 min at 25 °C in well plates. The fluorescence intensity produced by substrate hydrolysis was observed on a microplate reader with excitation and emission wavelengths of 545 and 590 nm, respectively. The inhibition ratio was obtained using the following equation:

$$\text{Inhibition (\%)} = [1 - (S - S_0)/(C - C_0)] \times 100$$

where C was the fluorescence of control (enzyme, assay buffer, and substrate) after 60 min of incubation, C_0 was the fluorescence of control at time 0, S was the fluorescence of tested samples (enzyme, sample solution, and substrate) after 60 min of incubation, and S_0 was the fluorescence of the tested samples at time 0.

A human recombinant TACE (0.1 ppm in 25 mM Tris buffer), the substrate (APP peptide YEVHHQKLV using EDANS/DABCYL), and samples were dissolved in an assay buffer, which were then combined and incubated for 60 min in the dark at 25 °C. The increase in fluorescence intensity produced by substrate hydrolysis was measured by using a microplate reader with excitation and emission wavelengths of 320 and 405 nm, respectively.

Absorbance assays for trypsin, chymotrypsin, and elastase were estimated using N-benzoyl-L-Arg-pNA, N-benzoyl-L-Tyr-pNA, and N-succinyl-Ala-Ala-Ala-pNA as substrates, respectively. Enzyme, Tris-HCl buffer (0.05 M, in 0.02 M $CaCl_2$, pH 8.2), and tested samples were incubated for 10 min at 25 °C then added to the substrate for 30 min at 37 °C. The absorbance was recorded at 410 nm. The inhibition ratio was obtained using the following equation:

$$\text{Inhibition (\%)} = \{[1 - (A - B)]/\text{control}\} \times 100$$

where A was the absorbance of control (enzyme, assay buffer, and substrate) after 60 min of incubation, and B was the absorbance of the tested sample (assay buffer and sample solution) after 60 min of incubation.

2.3. BACE1 Inhibition Kinetics

To determine the kinetic mechanisms of cardamonin, pinocembrin, and pinostrobin, Dixon and Lineweaver–Burk plots were used with varying concentrations of substrate (250, 500, and 750 nM) and inhibitors (0.1, 1, 5, 10, and 25 μM for cardamonin and 1, 10, 25, 37.5, and 50 μM for pinocembrin and pinostrobin). The dissociation constant (*Ki*) was obtained by Dixon plot and maximum reaction velocity (V_{max}) and Michaelis–Menten constant (K_m) values were determined by Lineweaver–Burk plot using SigmaPlot™ version 12.3 (Systat Software, Inc., San Jose, CA, USA).

2.4. In Silico Docking Studies

Molecular docking analysis of the interaction between BACE1 and our tested compounds was performed using the AutoDock Vina program to display the binding conformations of the compounds in the enzyme [28]. The amino acid sequence of BACE1 and P-glycoprotein (P-gp) (PDB, 2WJO and 3G60) was acquired from the Protein Data Bank (http://www.rcsb.org). The grid dimension was set to 30 Å × 30 Å × 30 Å with a cluster radius of 1 Å. The Cα coordinates for every used backbone-binding residue of the protein receptor were used for the center of docking space. Default options were selected for other docking simulations. The atomic coordinates of the ligands were drawn and visualized using Marvin sketch (5.11.4, 2012, ChemAxon, Cambridge, MA, USA). The calculated geometries were ranked in terms of the lowest energy, and the top-ranked poses were selected. The hydrogen bond calculation was evaluated using Chimera 10.0.2.

2.5. Statistics

All results were presented as the mean ± standard deviation (SD) of three independent experiments. Significant differences were determined by Duncan's multiple range tests using Statistical Analysis System (SAS) version 9.3 (Cary, NC, USA).

3. Results

3.1. Anti-BACE1 Activity of Cardamonin, Pinocembrin, and Pinostrobin

The structures of cardamonin (2′,4′-dihydroxy-6′-methoxychalcone), pinocembrin (5,7-dihydroxyflavanone), and pinostrobin (5-hydroxy-7methoxyflavanone) are shown in Figure 1. As depicted in Table 1, cardamonin presented the strongest BACE1 inhibition (IC$_{50}$, 4.35 ± 0.38 μM), followed by pinocembrin (IC$_{50}$, 27.01 ± 2.12 μM) and pinostrobin (IC$_{50}$, 28.44 ± 1.96 μM). In addition, the IC$_{50}$ value for cardamonin was three-fold higher than for resveratrol, which was used as a positive control.

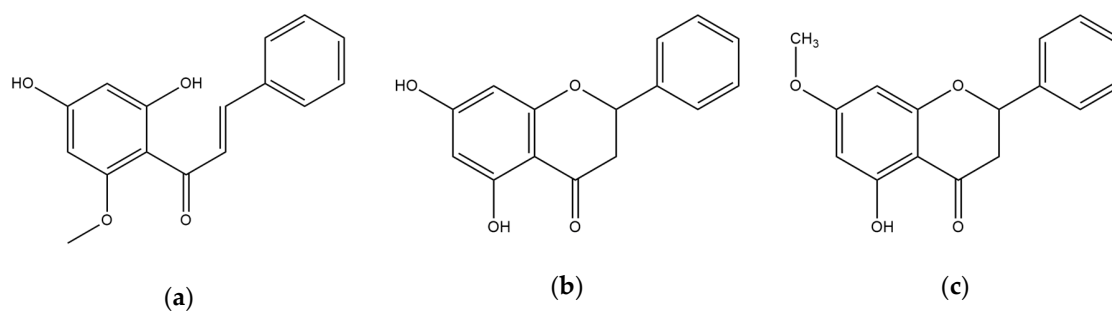**Figure 1.** The chemical structures of (**a**) cardamonin, (**b**) pinocembrin, and (**c**) pinostrobin.

To determine their specificity for BACE1, the compounds were tested on α-secretase (TACE), involved in non-amyloidogenic processes, as well as on other proteases. None of the three compounds significantly inhibited the activity of TACE or serine proteases, including trypsin, chymotrypsin, and elastase, even at a concentration of 100 μM (Table 2).

Table 1. Inhibitory activity and kinetic parameters of cardamonin, pinocembrin, and pinostrobin from *B. rotunda* against beta-site amyloid precursor protein cleaving enzyme1 (BACE1).

Compounds	Concentration (μM)	IC$_{50}$ (mean ± SD, μM) [1]	K$_m$	V$_{max}$	K$_i$ [2]	Inhibition Mode
Cardamonin	0.1 1 5 10 25	4.35 ± 0.38	833.3	1139 836 543 370 190	5.1	Noncompetitive
Pinocembrin	1 10 25 37.5 50	27.01 ± 2.12	312.5	507 471 336 270 229	29.3	Noncompetitive
Pinostrobin	1 10 25 37.5 50	28.44 ± 1.96	116.3	467 362 268 216 181	30.9	Noncompetitive
Resveratrol [3]		14.59 ± 0.79				

[1] The IC$_{50}$ values (μM) were calculated from a log dose inhibition curve and expressed as the mean ± SD. [2] K$_i$ has the dimension of a concentration with the unit of μmol/L (μM). [3] Resveratrol was used as a positive reference control in the BACE1.

Table 2. Inhibitory activities (%) of cardamonin, pinocembrin, and pinostrobin against α-secretase (tumor necrosis factor-α converting enzyme, TACE) and other serine proteases.

Sample (μM)	TACE	Trypsin	Chymotrypsin	Elastase
Cardamonin				
50	1.38 ± 0.36	1.13 ± 0.18	6.20 ± 0.41	2.29 ± 0.41
100	2.69 ± 1.44	3.74 ± 0.53	4.23 ± 0.55	1.41 ± 0.19
Pinocembrin				
10	5.15 ± 0.98	4.35 ± 0.26	7.18 ± 1.87	3.24 ± 0.19
100	6.95 ± 1.52	4.96 ± 0.27	8.61 ± 1.09	2.56 ± 0.08
Pinostrobin				
10	8.53 ± 1.05	3.19 ± 0.16	3.29 ± 0.25	5.21 ± 0.41
100	9.19 ± 1.20	1.52 ± 0.05	5.41 ± 0.49	2.63 ± 0.37

3.2. BACE1 Kinetics of Cardamonin, Pinocembrin, and Pinostrobin

The type of inhibition and kinetic analysis was determined using a Michaelis–Menten curve, Dixon plot, and Lineweaver–Burk plot (Figure 2). The three lines of the Dixon plots intersected on the x-axis of the same plot (Figure 2b,e,h). In addition, the Lineweaver–Burk plots showed decreased V$_{max}$ and unchanged K$_m$ at increasing inhibitor concentrations (Table 1). This pattern indicated non-competitive inhibitory activity against BACE1, thereby interacting with locations other than the active binding site for these compounds. For noncompetitive inhibition of enzymes, the K$_i$ value of inhibitor is essentially the same numerical value as the IC$_{50}$ [29]. As shown in Table 1, the K$_i$ values for cardamonin, pinocembrin, and pinostrobin were 5.1, 29.3, and 30.9 μM, respectively, which were similar to their IC$_{50}$ values. Because lower K$_i$ values represent tighter binding with the enzyme, cardamonin was determined to be the most potent BACE1 inhibitor of the three compounds tested.
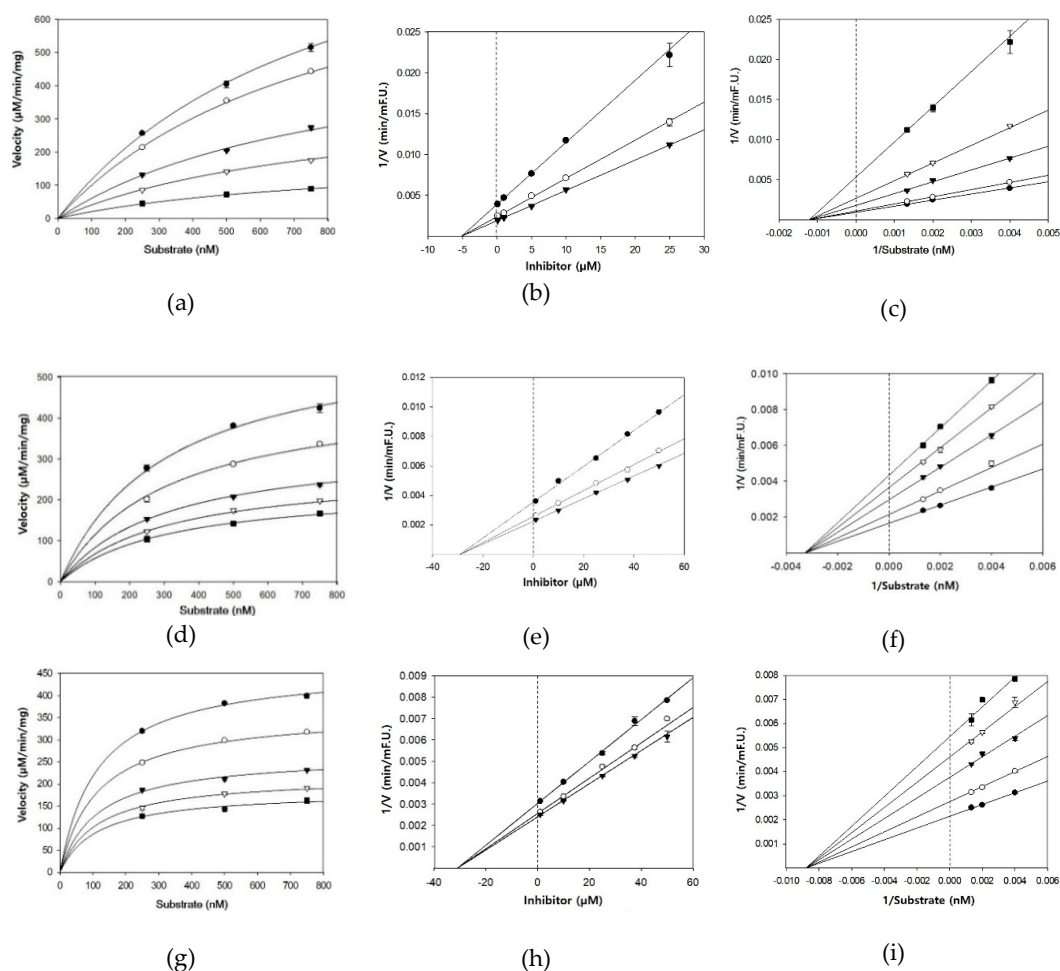
(a)

(b)

(c)

(d)

(e)

(f)

(g)

(h)

(i)

Figure 2. Michaelis–Menten plot of BACE1 inhibition by (**a**) cardamonin, (**d**) pinocembrin, and (**g**) pinostrobin in the presence of different inhibitor concentrations: 0.1 µM (●), 1 µM (○), 5 µM (▼), 10 µM (▽), and 25 µM (■) for cardamonin (a); 1 µM (●), 10 µM (○), 25 µM (▼), 37.5 µM (▽), and 50 µM (■) for pinocembrin (d) and pinostrobin (g). Dixon plot of BACE1 inhibition by (**b**) cardamonin, (**e**) pinocembrin, and (**h**) pinostrobin in the presence of different substrate concentrations: 250 nM (●), 500 nM (○), and 750 nM (▼). Lineweaver–Burk plot of BACE1 inhibition by (**c**) cardamonin, (**f**) pinocembrin, and (**i**) pinostrobin in the presence of different inhibitor concentrations: 0.1 µM (●), 1 µM (○), 5 µM (▼), 10 µM (▽), and 25 µM (■) for cardamonin (c); 1 µM (●), 10 µM (○), 25 µM (▼), 37.5 µM (▽), and 50 µM (■) for pinocembrin (f) and pinostrobin (i).

3.3. Molecular Docking Study of Cardamonin, Pinocembrin, and Pinostrobin with BACE1 and P-Glycoprotein (P-gp)

Based on the biological evaluation results, we performed molecular docking simulations of enzyme-inhibitor conformations and lowest binding energies. As indicated in Table 3, the docking results for cardamonin, pinocembrin, and pinostrobin showed negative binding energies of −9.5, −7.9, and −7.6 kcal/mol, respectively, suggesting that all our three compounds are high-affinity BACE1 inhibitors that can bind tightly to the enzyme. In addition, the pinocembrin-BACE1 complex was stabilized by the formation of a hydrogen bond between residue LYS75 and the hydroxyl group of pinocembrin at a distance of 3.088 Å (Figure 3d–f and Table 3). Pinostrobin is bound at the PHE108 residue of BACE1, connected by one hydrogen bond with a bonding distance of 1.990 Å (Figure 3g–i and Table 3). In cardamonin-BACE1 complex, Gln12, Leu30, Asp32, Val69, Tyr71, Lys75, Trp76, Phe108, Ile110, Trp115, and Gly230 of BACE1 participated in hydrophobic interactions with cardamonin without any hydrogen bonding interactions (Figure 3a–c and Table 3).

Table 3. Lowest energies and the number of hydrogen bond and hydrophobic interactions of cardamonin, pinocembrin, and pinostrobin with BACE1.

Ligands	Lowest Energy (kcal/mol)	No. of H-Bond	H-Bonds Interacting Residues	Bond Distance (Å)	van der Waals Interacting Residues
Cardamonin	−9.5				Gln12, Leu30, Asp32, Val69, Tyr71, Lys75, Trp76, Phe108, Ile110, Trp115, Gly230
Pinocembrin	−7.9	1	LYS 75	3.09	
Pinostrobin	−7.6	1	PHE 108	1.99	
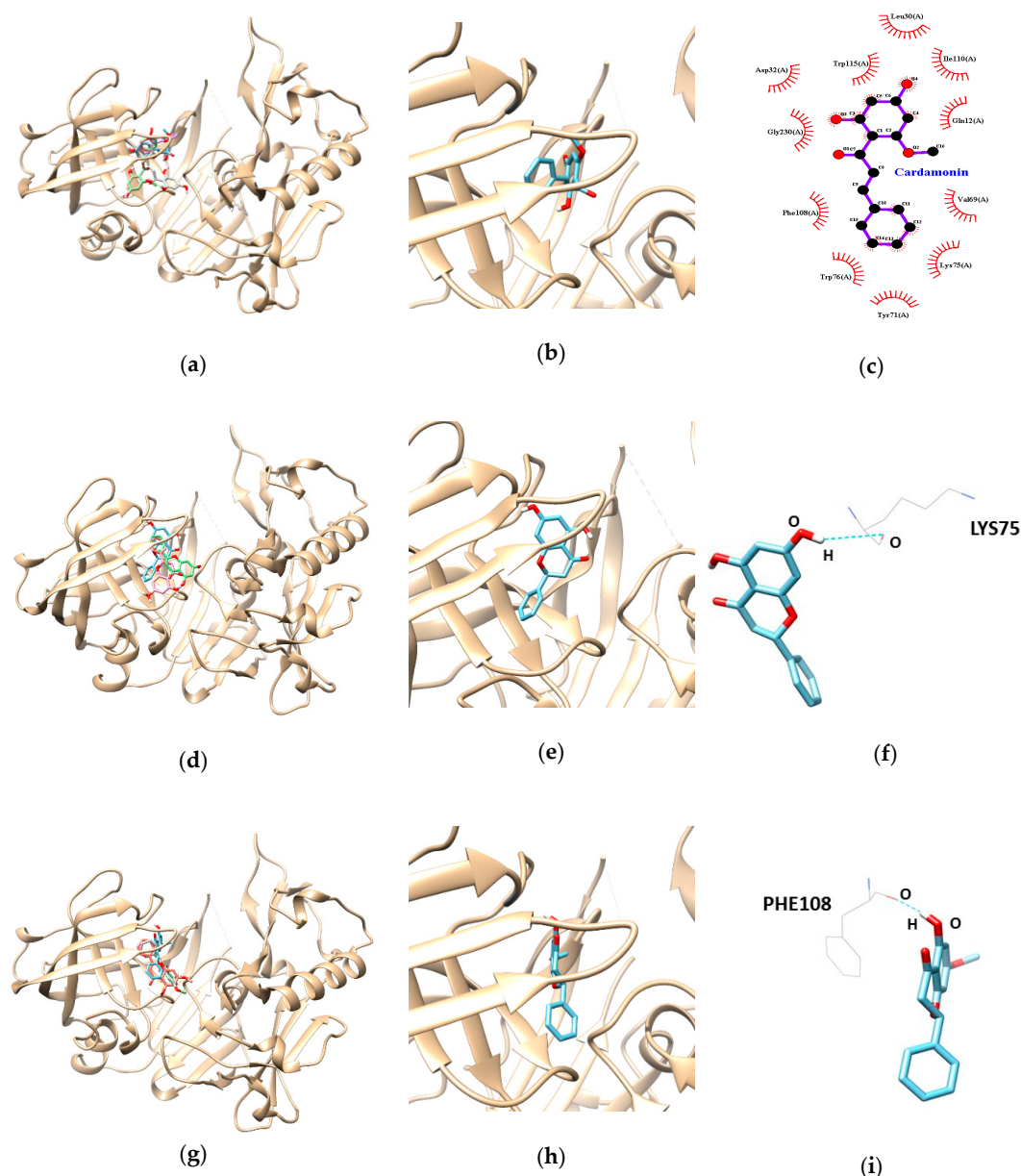
Figure 3. Molecular docking analysis of cardamonin, pinocembrin, and pinostrobin with BACE1. The best docking poses between BACE1 and cardamonin (**a**), pinocembrin (**d**), and pinostrobin (**g**). Magnified view of the binding site for cardamonin (**b**), pinocembrin (**e**), and pinostrobin (**h**). The hydrophobic interaction of cardamonin (**c**). Hydrogen interaction diagram of pinocembrin (**f**), and pinostrobin (**i**). The blue dotted lines show hydrogen bonds between ligands and BACE1.

The multidrug transporter P-glycoprotein (P-gp) is an important component of the BBB, acting as an ATP-driven efflux pump, controlling the movement of structurally diverse molecules across the BBB [30]. To predict the possibility of passing the BBB, the docking simulation between P-gp and our tested compounds was performed and the results are presented in Table 4 and Figure 4. Four hydrogen bonds were found between cardamonin and the P-gp residues, with the lowest binding energy of −9.78 kcal/mol. In addition, Tyr303, Gln721, and Ser725 participated in hydrogen-interactions (bonding distances of 3.17, 2.82, 3.25, and 2.96 Å, respectively). The pinocembrin-P-gp complex (the lowest binding energy: −10.64 kcal/mol) was stabilized by a hydrogen bond at Ser725 and Ser975 (bonding distance: 2.90 and 3.06 Å, respectively). Like pinocembrin, pinostrobin formed two hydrogen bonds with Ser725 and Ser975 (bonding distance: 2.89 and 3.03 Å, respectively).

Table 4. Lowest energies and the number of hydrogen and hydrophobic bond interactions of cardamonin, pinocembrin, and pinostrobin with P-glycoprotein (P-gp).

| Ligands	Lowest Energy (kcal/mol)	No. of H-Bond	H-Bonds Interacting Residues	Bond distance (Å)	van der Waals Interacting Residues
Cardamonin	−9.78	4	Tyr303, Gln721, Ser725	3.17 2.82 and 3.25 2.96	Phe71, Phe332, Phe724, Phe728, Leu971, Phe974, Ser975, Val978
Pinocembrin	−10.64	2	Ser725, Ser975	2.90 3.06	Phe71, Phe332, Phe724, Phe728, Phe953, Leu971, Phe974, Val978
Pinostrobin	−10.37	2	Ser725,Ser975	2.89 3.03	Phe71, Phe332, Phe724, Phe728, Phe953, Leu971, Phe974, Val978

(**a**)

(**b**)

(**c**)
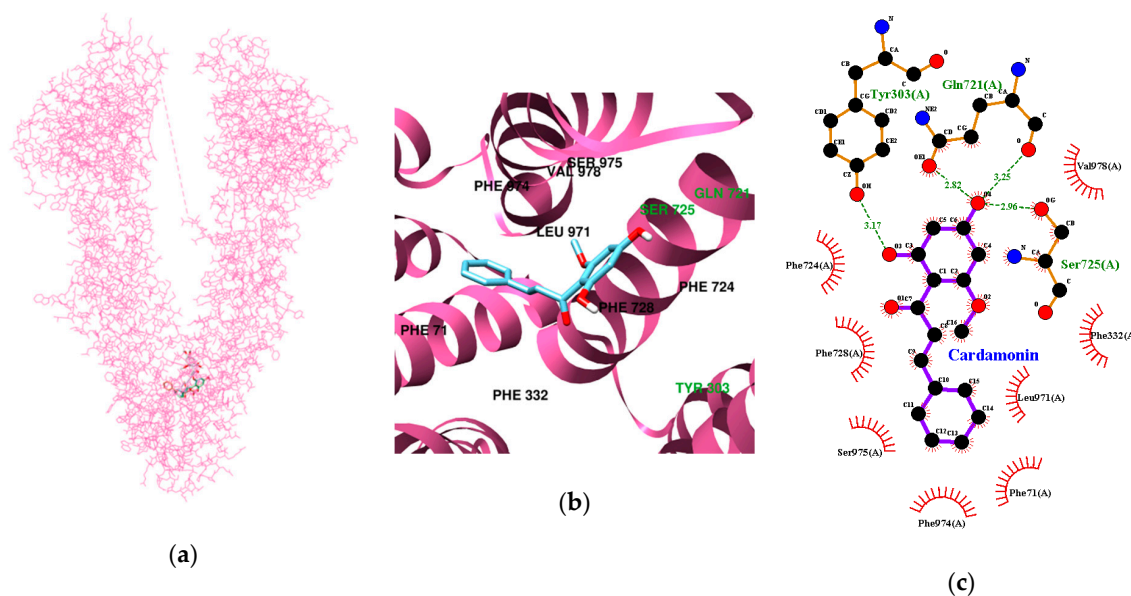
Figure 4. *Cont.*
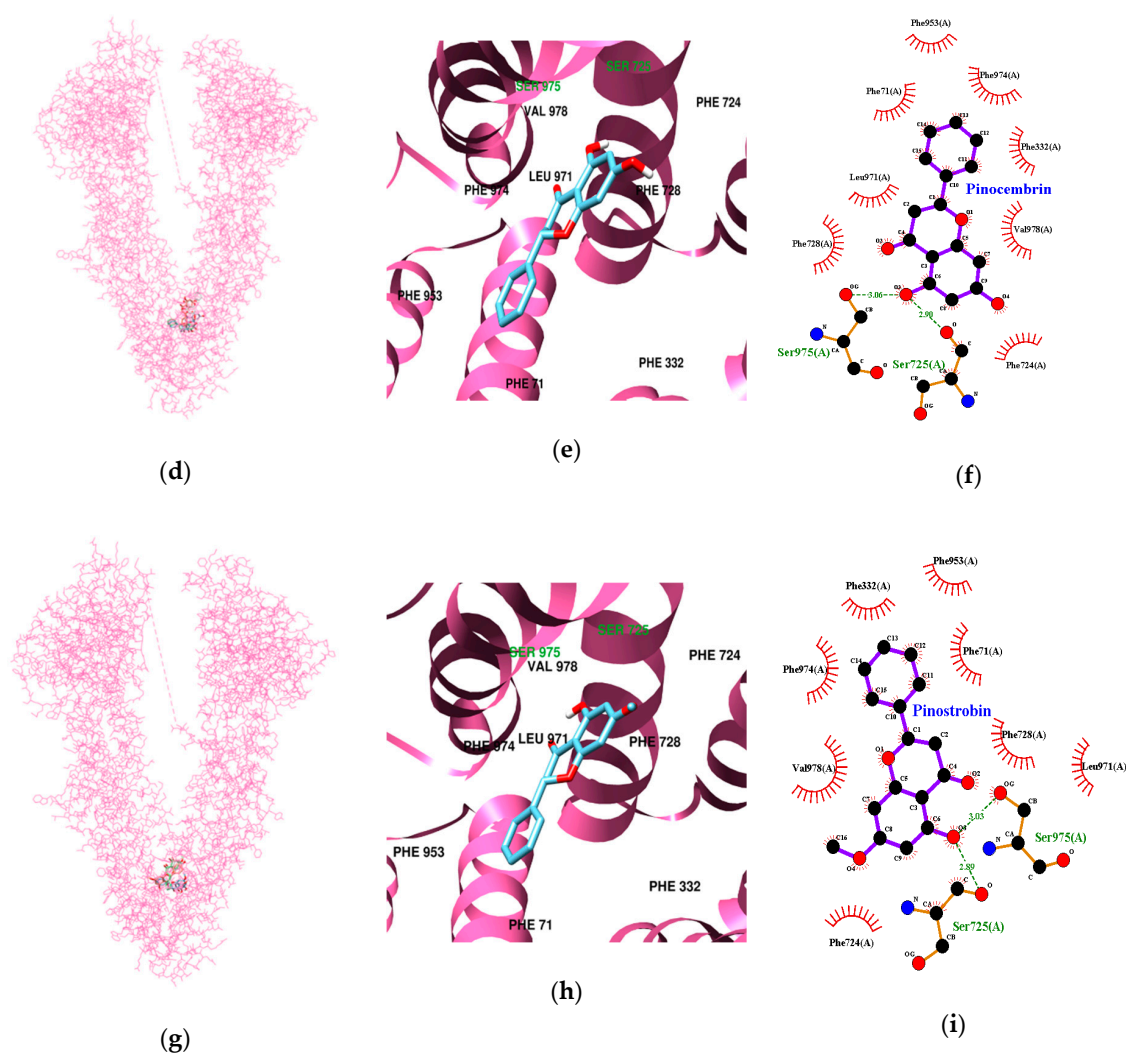
Figure 4. Molecular docking analysis of cardamonin, pinocembrin, and pinostrobin with P-gp. The best docking poses between P-gp and cardamonin (**a**), pinocembrin (**d**), and pinostrobin (**g**). Magnified view of the binding site for cardamonin (**b**), pinocembrin (**e**), and pinostrobin (**h**). Hydrogen and hydrophobic interaction diagram of cardamonin (**c**), pinocembrin (**f**), and pinostrobin (**i**). The green dotted lines show hydrogen bonds between ligands and BACE1.

4. Discussion

In the present study, we investigated the anti-AD potential of three flavonoids from *B. rotunda*, namely cardamonin, pinocembrin, and pinostrobin, by evaluating their capacity to inhibit BACE1. These compounds exhibited powerful inhibitory activities on BACE1 with IC_{50} values in the range of 4.4–28.4 μM. Several other natural BACE1 inhibitors including genistein, biochanin A, daidzein, formononetin, and glycitein had IC_{50} values ranging from at a range of 28->100 μM [27,31]. The results showed that cardamonin, containing an α, β-unsaturated ketone with two aromatic rings, was the most potent BACE1 inhibitor of the three flavonoids. Similar results for the correlation between structure and enzyme inhibition properties were shown in a previous study [32]. Using an antiviral assay, the authors showed that cardamonin exhibited the strongest inhibition of HIV-1 protease activity, with an IC_{50} value of 31.0 μg/mL, compared to pinocembrin (>100 μg/mL) and pinostrobin (>100 μg/mL). Further enzyme kinetic evaluations using various substrates and inhibitor concentrations indicated that all three compounds are noncompetitive BACE1 inhibitors. The docking results indicated that hydrogen bond formation played a key role in the interaction of pinocembrin and pinostrobin with BACE1. However, cardamonin did not form any hydrogen bonds with BACE1 even though it presented the

strongest BACE1 inhibition, suggesting that hydrophobic bonds were involved in the interaction between this compound and BACE1. The cardamonin result is in agreement with the report by Castro et al. (2015), which showed that cardamonin inhibited SmATPDase 1 through hydrophobic interactions [33].

Together, the above results indicate that all three compounds are beneficial BACE1 inhibitors, with potential as candidates for use in the prevention and/or treatment of AD. However, few BACE1 inhibitors have been marketed to treat AD due to the difficulty in developing therapeutic agents that can efficiently cross the BBB and reach appropriate concentrations in the cerebral parenchyma, and, moreover, can do so without side effects [34]. Recently, QSAR study approaches have been used to generate predictive models for BBB permeability. To cross the BBB, an active compound must possess the following physicochemical properties: a molecular weight (MW) of less than 450, polar surface area (PSA) of less than 70 Å^2, and a clog *P* value, used as an assessment of lipophilicity, between 0 and 5 [35]. Cardamonin has a MW of 270.28, a PSA value calculated as 66.76, and a clog *P* of 4.54, obtained by determining the partition coefficient between n-octanol and water [19]. Furthermore, a previous study showed that some synthetic indolyl chalcones could cross the BBB, as determined by a parallel artificial membrane permeability assay [36]. Therefore, cardamonin is predicted to cross the BBB and exert its activity in the brain. An in vitro study by Yang et al. demonstrated that pinocembrin could cross the BBB by passive transport partly through P-glycoprotein [37].

Abnormal phosphorylated tau protein promotes the loss of microtubule-stabilizing ability and may contribute to neuronal degeneration as well as NFT formation [38]. To date, however, it is not known whether our three flavonoids can inhibit tau phosphorylation. However, several studies have revealed aspects in regard to the effect of flavonoids on the tau protein. Myricetin and epicatechin-5-gallate have been shown to suppress heparin-induced tau production and administration of EGCG leads to regulated tau profiles in AD transgenic mouse model, with inhibition of sarkosyl-soluble phosphorylated tau isoforms [39,40]. The authors plan to examine the attenuation effect of the three flavonoids on tau pathology in future studies.

Chronic oral administration of cardamonin (10 mg/kg) for 30 weeks did not elicit any apparent toxicity [41]. Additionally, Charoensin et al. reported that pinostrobin and pinocembrin also did not induce any toxicity or mutagenic effects following oral administration of 100 mg/kg for 7 days in Wister rats, suggesting that all three compounds are safe for consumption [42].

Overall, our tested compounds appear to be safe and potent natural BACE1 inhibitors that hold promise for use in the prevention and/or treatment of AD.

5. Conclusions

To the best of our knowledge, the present study is the first to indicate that cardamonin, pinocembrin, and pinostrobin are potent and selective BACE1 inhibitors. In a biological study, cardamonin was six-fold more effective than the two flavanones, pinocembrin and pinostrobin, at inhibiting BACE1. In addition, the inhibition kinetics and docking studies confirmed the allosteric nature of BACE1 inhibition by the tested compounds. Although further in vivo studies of these compounds are required to confirm our present results, our compounds may be good candidates for development as preventative agents against AD through inhibition of Aβ formation.

Author Contributions: K.Y. carried out biological experiments and data analysis. M.J. supervised the experimental work and data analysis and wrote the manuscript.

Conflicts of Interest: The authors declare no conflict of interest.

References

1. Selkoe, D. Alzheimer's disease results from the cerebral accumulation and cytotoxicity of amyloid beta-protein. *J. Alzheimer's Dis.* **2001**, *3*, 75–80. [CrossRef]

2. LaFerla, F. Pathways linking Abeta and tau pathologies. *Biochem. Soc. Trans.* **2010**, *38*, 993–995. [CrossRef] [PubMed]

3. Haass, C.; Selkoe, D. Soluble protein oligomers in neurodegeneration: Lessons from the Alzheimer's amyloid beta-peptide. *Nat. Rev. Mol. Cell Biol.* **2007**, *8*, 101–112. [CrossRef] [PubMed]

4. Sadigh-Eteghad, S.; Sabermarouf, B.; Majdi, A.; Talebi, M.; Farhoudi, M.; Mahmoudi, J. Amyloid-beta: A crucial factor in Alzheimer's disease. *Med. Princ. Pract.* **2015**, *24*, 1–10. [CrossRef]

5. Zhao, H.; Wang, S.L.; Qian, L.; Jin, J.L.; Li, H.; Xu, Y.; Zhu, X.-L. Diammonium glycyrrhizinate attenuates Abeta(1–42)-induced neuroinflammation and regulates MAPK and NF-κB pathways in vitro and in vivo. *CNS Neurosci. Ther.* **2013**, *19*, 117–124. [CrossRef] [PubMed]

6. Botteri, G.; Salvadó, L.; Gumà, A.; Lee Hamilton, D.; Meakin, P.; Montagut, G.; Ashford, M.; Ceperuelo-Mallafré, V.; Fernández-Veledo, S.; Vendrell, J.; et al. The BACE1 product sAPPβ induces ER stress and inflammation and impairs insulin signaling. *Metabolism* **2018**, *85*, 59–75. [CrossRef] [PubMed]

7. Panza, F.; Frisardi, V.; Imbimbo, B.; Capurso, C.; Logroscino, G.; Sancarlo, D.; Seripa, D.; Vendemiale, G.; Pilotto, A.; Solfrizzi, V. REVIEW: γ-Secretase inhibitors for the treatment of Alzheimer's disease: The current state. *CNS Neurosci. Ther.* **2010**, *16*, 272–284. [CrossRef] [PubMed]

8. Hu, X.; Hicks, C.; He, W.; Wong, P.; Macklin, W.; Trapp, B.; Yan, R. Bace1 modulates myelination in the central and peripheral nervous system. *Nat. Neurosci.* **2006**, *9*, 1520–1525. [CrossRef] [PubMed]

9. Savonenko, A.; Melnikova, T.; Laird, F.; Stewart, K.; Price, D.; Wong, P. Alteration of BACE1- dependent NRG1/ErbB4 signaling and schizophrenia-like phenotypes in BACE1-null mice. *Proc. Natl. Acad. Sci. USA* **2008**, *105*, 5585–5590. [CrossRef] [PubMed]

10. Ghosh, A.; Brindisi, M.; Tang, J. Developing beta-secretase inhibitors for treatment of Alzheimer's disease. *J. Neurochem.* **2012**, *120*, 71–83. [CrossRef] [PubMed]

11. Yan, R.; Vassar, R. Targeting the β secretase BACE1 for Alzheimer's disease therapy. *Lancet Neurol.* **2014**, *13*, 319–329. [CrossRef]

12. Yan, R. Stepping closer to treating Alzheimer's disease patients with BACE1 inhibitor drugs. *Transl. Neurodegener.* **2016**, *5*, 13–23. [CrossRef] [PubMed]

13. Vassar, R. BACE1 inhibitor drugs in clinical trials for Alzheimer's disease. *Alzheimers Res. Ther.* **2014**, *6*, 89–102. [CrossRef]

14. Eng-Chong, T.; Yean-Kee, L.; Chin-Fei, C.; Choon-Han, H.; Sher-Ming, W.; Thio Li-Ping, C.; Gen-Teck, F.; Khalid, N.; Rahman, N.; Karsani, S.; et al. *Boesenbergia rotunda*: From Ethnomedicine to Drug Discovery. *Evid. Based Complement. Alternat. Med.* **2012**, 1–25. [CrossRef]

15. Kirana, C.; Jones, G.; Record, I.; McIntosh, G. Anticancer properties of panduratin A isolated from *Boesenbergia pandurata* (Zingiberaceae). *J. Nat. Med.* **2007**, *61*, 131–137. [CrossRef]

16. Roy, A.; Bharadvaja, N. Medicinal Plants in the Management of Cancer: A Review. *Int. J. Complement. Alt. Med.* **2017**, *9*, 009291.

17. Xian, Y.; Ip, S.; Lin, Z.; Mao, Q.; Su, Z.; Lai, X. Protective effects of pinostrobin on β-amyloid-induced neurotoxicity in PC12 cells. *Cell Mol. Neurobiol.* **2012**, *32*, 1223–1230. [CrossRef]

18. Chow, Y.; Lee, K.; Vidyadaran, S.; Lajis, N.; Akhtar, M.; Israf, D.; Syahida, A. Cardamonin from Alpinia rafflesiana inhibits inflammatory responses in IFN-γ/LPS-stimulated BV2 microglia via NF-κB signalling pathway. *Int. Immunopharmacol.* **2012**, *12*, 657–665. [CrossRef]

19. Peng, S.; Hou, Y.; Yao, J.; Fang, J. Activation of Nrf2-driven antioxidant enzymes by cardamonin confers neuroprotection of PC12 cells against oxidative damage. *Food Funct.* **2017**, *8*, 997–1007. [CrossRef]

20. Liu, R.; Gao, M.; Yang, Z.H.; Du, G.H. Pinocembrin protects rat brain against oxidation and apoptosis induced by ischemia-reperfusion both in vivo and in vitro. *Brain Res.* **2008**, *1216*, 104–115. [CrossRef]

21. Jin, X.; Liu, Q.; Jia, L.; Li, M.; Wang, X. Pinocembrin attenuates 6-OHDA-induced neuronal cell death through Nrf2/ARE pathway in SH-SY5Y cells. *Cell Mol. Neurobiol.* **2015**, *35*, 323–333. [CrossRef]

22. Wang, Y.; Miao, Y.; Mir, A.; Cheng, L.; Wang, L.; Zhao, L.; Cui, Q.; Zhao, W.; Wang, H. Inhibition of beta-amyloid-induced neurotoxicity by pinocembrin through Nrf2/HO-1 pathway in SH-SY5Y cells. *J. Neurol. Sci.* **2016**, *368*, 223–230. [CrossRef]

23. Saad, M.; Abdel Salam, R.; Kenawy, S.; Attia, A. Pinocembrin attenuates hippocampal inflammation, oxidative perturbations and apoptosis in a rat model of global cerebral ischemia reperfusion. *Pharmacol. Rep.* **2015**, *67*, 115–122. [CrossRef]

24. Liu, R.; Wu, C.; Zhou, D.; Yang, F.; Tian, S.; Zhang, L.; Zhang, T.; Du, G. Pinocembrin protects against β-amyloid-induced toxicity in neurons through inhibiting receptor for advanced glycation end products (RAGE)-independent signaling pathways and regulating mitochondrion-mediated apoptosis. *BMC Med.* **2012**, *10*, 105–126. [CrossRef]

25. Liu, R.; Li, J.; Song, J.; Zhou, D.; Huang, C.; Bai, X.; Xie, T.; Zhang, X.; Li, Y.; Wu, C.; et al. Pinocembrin improves cognition and protects the neurovascular unit in Alzheimer related deficits. *Neurobiol. Aging* **2014**, *35*, 1275–1285. [CrossRef]

26. Li, C.; Tang, B.; Feng, Y.; Tang, F.; Pui-Man Hoi, M.; Su, Z.; Ming-Yuen Lee, S. Pinostrobin Exerts Neuroprotective Actions in Neurotoxin-Induced Parkinson's Disease Models through Nrf2 Induction. *J. Agric. Food Chem.* **2018**, *66*, 8307–8318. [CrossRef]

27. Youn, K.; Park, J.H.; Lee, J.; Jeong, W.S.; Ho, C.T.; Jun, M. The Identification of Biochanin A as a Potent and Selective β-Site App-Cleaving Enzyme 1 (Bace1) Inhibitor. *Nutrients* **2016**, *8*, 637. [CrossRef]

28. Trott, O.; Olson, A. AutoDock Vina: Improving the speed and accuracy of docking with a new scoring function, efficient optimization and multithreading. *J. Comput. Chem.* **2010**, *31*, 455–461. [CrossRef]

29. Cheng, Y.; Prusoff, W. Relationship between the inhibition constant (K1) and the concentration of inhibitor which causes 50 per cent inhibition (I50) of an enzymatic reaction. *Biochem. Pharmacol.* **1973**, *22*, 3099–3108.

30. Mizutani, T.; Nakamura, T.; Morikawa, R.; Fukuda, M.; Mochizuki, W.; Yamauchi, Y.; Nozaki, K.; Yui, S.; Nemoto, Y.; Nagaishi, T.; et al. Real-time analysis of P-glycoprotein-mediated drug transport across primary intestinal epithelium three-dimensionally cultured in vitro. *Biochem. Biophys. Res. Commun.* **2012**, *419*, 238–243. [CrossRef]

31. Youn, K.; Park, J.; Lee, S.; Lee, S.; Lee, J.; Yun, E.; Jeong, W.; Jun, M. BACE1 Inhibition by Genistein: Biological Evaluation, Kinetic Analysis, and Molecular Docking Simulation. *J. Med. Food* **2018**, *21*, 416–420. [CrossRef]

32. Tewtrakul, S.; Subhadhirasakul, S.; Puripattanavong, J.; Panphadung, T. HIV-1 protease inhibitory substances from the rhizomes of *Boesenbergia pandurata* Holtt. *Songklanakarin J. Sci. Technol.* **2003**, *25*, 6–11.

33. De Castro, C.; Costa, P.; Laktin, G.; de Carvalho, P.; Geraldo, R.; de Moraes, J.; Pinto, P.; Couri, M.; Pinto Pde, F.; Da Silva Filho, A. Cardamonin, a schistosomicidal chalcone from *Piper aduncum* L. (Piperaceae) that inhibits Schistosoma mansoni ATP diphosphohydrolase. *Phytomedicine* **2015**, *22*, 921–928. [CrossRef] [PubMed]

34. Hayes, M. Bioactive peptides and their potential use for the prevention of diseases associated with Alzheimer's disease and mental health disorders. *Ann. Psychiatry Ment. Health* **2014**, *2*, 1017–1025.

35. Pajouhesh, H.; Lenz, G. Medicinal chemical properties of successful central nervous system drugs. *NeuroRx* **2005**, *2*, 541–553. [CrossRef]

36. Sasidharan, R.; Manju, S.; Uçar, G.; Baysal, I.; Mathew, B. Identification of Indole-Based Chalcones: Discovery of a Potent, Selective, and Reversible Class of MAO-B Inhibitors. *Arch. Pharm. (Weinh.)* **2016**, *349*, 627–637. [CrossRef] [PubMed]

37. Yang, Z.; Sun, X.; Qi, Y.; Mei, C.; Sun, X.; Du, G. Uptake characteristics of pinocembrin and its effect on p-glycoprotein at the blood-brain barrier in in vitro cell experiments. *J. Asian Nat. Prod. Res.* **2012**, *14*, 14–21. [CrossRef]

38. Goedert, M.; Crowther, R.; Spillantini, M. Tau mutations cause frontotemporal dementias. *Nueron* **1998**, *21*, 955–958. [CrossRef]

39. Taniguchi, S.; Suzuki, N.; Masuda, M.; Hisanaga, S.; Iwatsubo, T.; Goedert, M.; Hasegawa, M. Inhibition of heparin-induced tau filament formation by phenothiazines, polyphenols, and porphyrins. *J. Biol. Chem.* **2005**, *280*, 7614–7623. [CrossRef] [PubMed]

40. Rezai-Zadeh, K.; Arendash, G.; Hou, H.; Fernandez, F.; Jensen, M.; Runfeldt, M.; Shytle, R.; Tan, J. Green tea epigallocatechin-3-gallate (EGCG) reduces beta-amyloid mediated cognitive impairment and modulates tau pathology in Alzheimer transgenic mice. *Brain Res.* **2008**, *1214*, 177–187. [CrossRef] [PubMed]

41. James, S.; Aparna, J.; Paul, A.; Lankadasari, M.; Mohammed, S.; Binu, V.; Santhoshkumar, T.; Reshmi, G.; Harikumar, K. Cardamonin inhibits colonic neoplasia through modulation of MicroRNA expression. *Sci. Rep.* **2017**, *7*, 13945. [CrossRef] [PubMed]

42. Charoensin, S.; Punvittayagul, C.; Pompimon, W.; Mevatee, U.; Wongpoomchai, R. Toxicological and clastogenic evaluation of pinocembrin and pinostrobin isolated from *Boesenbergia pandurata* in Wistar rats. *Thai J. Toxicol.* **2010**, *25*, 29–40.